

Soft Diffraction at the LHC¹

V.A. Khoze^{a,b}, A.D. Martin^a and M.G. Ryskin^{a,b}

^a Institute for Particle Physics Phenomenology, University of Durham, Durham, DH1 3LE

^b Petersburg Nuclear Physics Institute, Gatchina, St. Petersburg, 188300, Russia

Abstract

We present a triple-Regge analysis of the available $pp \rightarrow p + X$ high-energy data accounting for absorptive corrections. We describe a model for high-energy soft interactions which includes the whole set of multi-Pomeron ($n \rightarrow m$) vertices, and give predictions for the LHC.

1 Motivation

There are two main reasons for revisiting soft pp high energy interactions at this time.

A. To predict soft processes at the LHC we need a reliable model. A detailed analysis performed in the late sixties [1, 2] showed that there could be different scenarios for the high-energy behaviour of the interaction amplitude.

In the ‘weak coupling’ regime the total cross section $\sigma_t(s \rightarrow \infty) \rightarrow \text{const}$, and in order not to violate unitarity, and to satisfy the inequality

$$\sigma^{SD} = \int \frac{d\sigma^{SD}}{dM^2} dM^2 < \sigma_t, \quad (1)$$

the triple-Pomeron vertex must vanish when $t \rightarrow 0$, that is $g_{3P} \propto t$. In this case, the large logarithm coming from the integration over the mass of the system produced in diffractive

dissociation ($\int dM^2/M^2 \simeq \ln s$) is compensated by the small value of the mean momentum transferred through the Pomeron $\langle t \rangle \propto 1/\ln s$.

On the other hand, for ‘strong coupling’, with $\sigma_t \propto (\ln s)^\eta$ with $0 < \eta \leq 2$, the inequality (1) is provided by a small value of the rapidity gap survival factor S^2 which decreases with energy.

The present diffractive data are better described within the ‘strong coupling’ approach, and here we show predictions for the LHC for this scenario. However, the possibility of the ‘weak coupling’ scenario is not completely excluded yet. Therefore, it is quite important to study the different channels of diffractive dissociation at the LHC in order to reach a final conclusion and to fix the parameters of the model for high-energy soft interactions.

B. The second reason for studying soft interactions arises because it may not be an easy task to distinguish the production of a new object at the LHC when it is accompanied by hundreds other particles emitted in the same event. For the detailed study of the new object, A , it may be better to select the few, very clean, events with the Large Rapidity Gaps (LRG) on either side of the new object [3]. That is to observe the exclusive process $pp \rightarrow p + A + p$. In such a Central Exclusive Process (CEP) the mass of A can be measured with very good accuracy ($\Delta M_A \sim 1 - 2$ GeV) by the missing-mass method by detecting the outgoing forward protons. Moreover, a specific $J_z = 0$ selection rule [4] reduces the background and also greatly simplifies the spin-parity analysis of A . However, the CEP cross section is strongly suppressed by the small survival factor, $S^2 \ll 1$, of the rapidity gaps. Thus we need a reliable model of soft interactions to evaluate the corresponding value of S^2 .

2 Triple-Regge analysis accounting for absorptive effects

The total and elastic proton-proton cross sections are usually described in terms of an eikonal model, which automatically satisfies s -channel elastic unitarity. To account for the possibility of excitation of the initial proton, that is for two-particle intermediate states with the proton replaced by N^* , we use the Good-Walker formalism [5]. Already at Tevatron energies the absorptive correction to the elastic amplitude, due to elastic eikonal rescattering, is not negligible; it is about 20% in comparison with the simple one Pomeron exchange. After accounting for low-mass proton excitations (that is N^* ’s in the intermediate states) the correction becomes twice larger (that is, up to 40%). Next, in order to describe high-mass diffractive dissociation, $d\sigma^{SD}/dM^2$, we have to include an extra factor of 2 from the AGK cutting rules [6]. Thus, the absorptive effects in the triple-Regge domain are expected to be quite large. The previous triple-Regge analyses (see, for example, [7]) did not allow for absorptive corrections and the resulting triple-Regge couplings must be regarded, not as bare vertices, but as effective couplings embodying the absorptive effects. Since the inelastic cross section (and, therefore, the absorptive corrections) expected at the LHC are more than twice as large as that observed at fixed-target and CERN-ISR energies, the old triple-Regge vertices cannot be used to predict

the diffractive cross sections at the LHC. Thus, it is necessary to perform a new triple-Regge analysis that includes the absorptive effects explicitly.

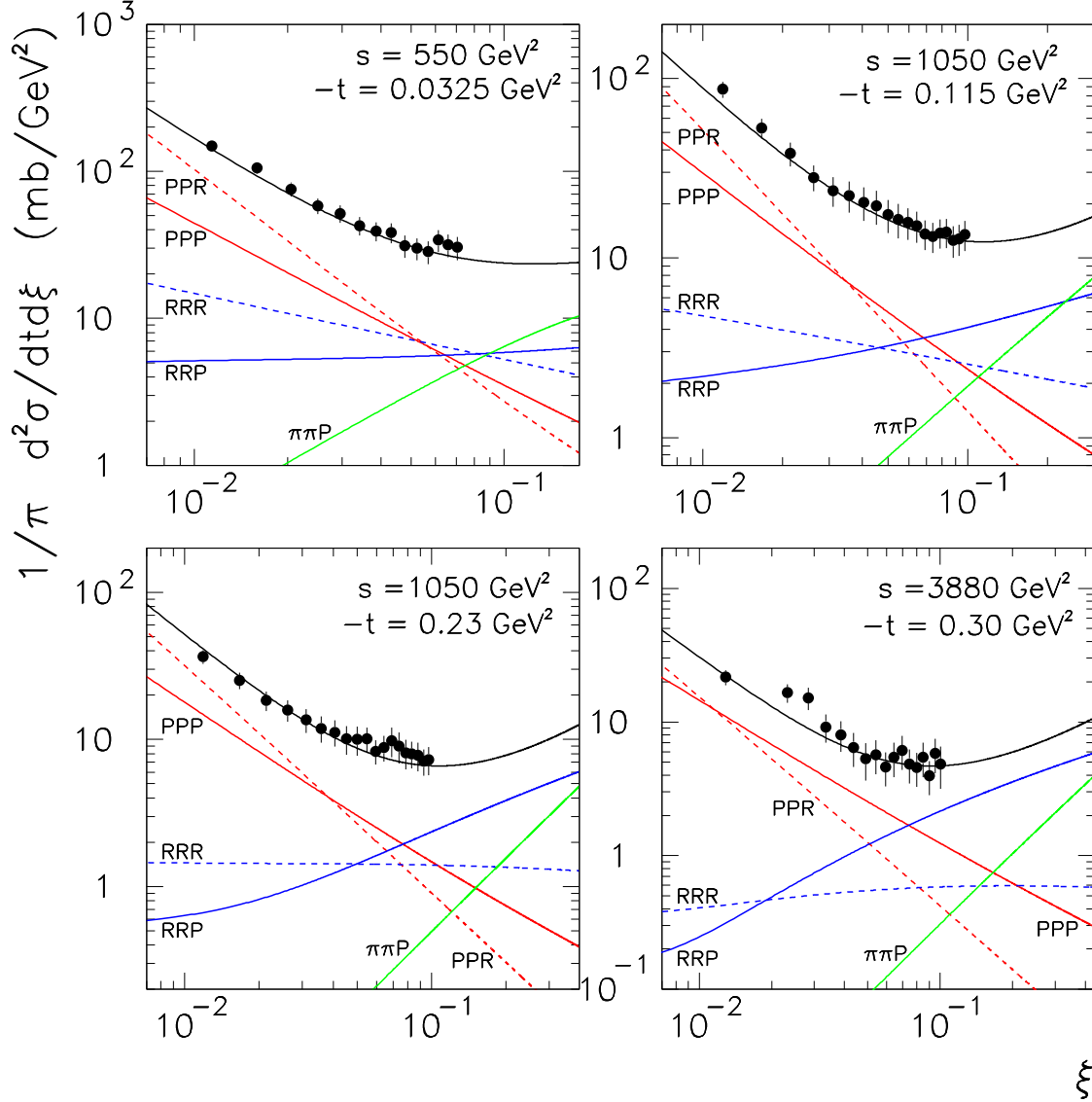


Figure 1: The description of the CERN-ISR $pp \rightarrow pX$ cross section $d\sigma/dtd\xi$ data obtained in the strong triple-Pomeron coupling fit, where $\xi = M^2/s$. The individual triple-Regge contributions are also shown.

Together with E.G.D.S.Luna, we fitted [8] the fixed-target FNAL, CERN-ISR and Tevatron data that are available in the triple-Regge region. We included ‘ PPP ’, ‘ PPR ’, ‘ RRP ’, ‘ RRR ’ and $\pi\pi P$ contributions, assuming either the ‘strong’ or ‘weak’ coupling scenarios for the behaviour of the triple-Pomeron vertex. To account for the absorptive corrections we used a two-channel (Good-Walker) eikonal model, which describes well the total, σ_t , and elastic, $d\sigma_{el}/dt$, pp and $\bar{p}p$ cross sections.

In the ‘strong’ coupling case, a good $\chi^2/\text{DoF}=167/(210-8)=0.83$ was obtained. The quality of the description to a sample of the data can be seen in Fig.1, where the various triple-Regge contributions to the cross section are also shown. In comparison with the old triple-Regge analysis [7], we now have about a twice larger relative contribution of the ‘*PPR*’ term. This is mainly due to the inclusion in our analysis of the higher-energy Tevatron data.

Since the absorptive effects are included explicitly, the extracted values of the triple-Reggeon vertices are now much closer to the *bare* triple-Regge couplings. In particular, the value

$$g_{PPP} \simeq 0.2g_N \quad (2)$$

is consistent with a reasonable extrapolation of the perturbative BFKL Pomeron vertex to the low scale region [9]; here g_N is the Pomeron-proton coupling. Note also that these values of ‘*PPP*’ and ‘*PPR*’ vertices allow us to describe the HERA data [10] on inelastic J/ψ photoproduction, $\gamma p \rightarrow J/\psi + Y$, where the screening corrections are rather small.

The ‘weak’ coupling scenario leads to a larger $\chi^2/\text{DoF}=1.4$ and to a worse description of the $\gamma p \rightarrow J/\psi + Y$ process at the lowest values of t . At the LHC energy the ‘weak’ coupling fit predicts about 3 times smaller inclusive cross section $d\sigma^{SD}/dt dM^2$ at $\xi = M^2/s = 0.01$ in comparison with that predicted in the ‘strong’ coupling case.

3 Model with the whole set of multi-Pomeron vertices

Since the triple-Pomeron vertex (2) turns out to be rather large, the contribution of the so-called ‘enhanced’ diagrams, with a few vertices, is not negligible. Moreover, we cannot expect that more complicated multi-Pomeron interactions, driven by the g_m^n vertices, which describe the transition of n to m Pomerons, will not affect the final result. It looks more reasonable to assume that $g_m^n \propto \lambda^{n+m}$ than to assume that $g_m^n = 0$ for any $n + m > 3$. Thus we need a model which accounts for the possibility of multi-Pomeron interactions (with arbitrary n and m).

While the eikonal formalism describes the rescattering of the incoming fast particles, the enhanced multi-Pomeron diagrams represent the rescattering of the intermediate partons in the ladder (Feynman diagram) which describes the Pomeron-exchange amplitude. The ladder-type Pomeron amplitude may be generated by the evolution equation (in rapidity, y , space)

$$\frac{d\Omega(y, b)}{dy} = \left(\Delta + \alpha' \frac{d^2}{d^2 b} \right) \Omega(y, b) \quad (3)$$

where b is the two-dimensional vector in impact parameter space and α' is the slope of the Pomeron trajectory. Δ is the probability to emit new intermediate partons within unit rapidity interval; the Pomeron intercept $\alpha(0) = 1 + \Delta$. The solution of (3), $\Omega = \Omega_0 \exp(\Delta y - b^2/4\alpha'y)/4\pi\alpha'y$, is the opacity (at point y, b), corresponding to the incoming particle placed at $b = 0$ and $y = 0$.

It looks natural to account for absorptive effects by including on the r.h.s. of (3) the factor $\exp(-\lambda\Omega_i/2 - \lambda\Omega_k/2)$, where the subscripts i and k denote the opacities of the beam and the target incoming hadrons. We thus have the evolution equations

$$\frac{d\Omega_i(y, b)}{dy} = \exp(-\lambda\Omega_i(y, b)/2 - \lambda\Omega_k(y', b)/2) \left(\Delta + \alpha' \frac{d^2}{d^2b} \right) \Omega_i(y, b) \quad (4)$$

$$\frac{d\Omega_k(y', b)}{dy'} = \exp(-\lambda\Omega_i(y, b)/2 - \lambda\Omega_k(y', b)/2) \left(\Delta + \alpha' \frac{d^2}{d^2b} \right) \Omega_k(y', b), \quad (5)$$

where here $y' = \ln s - y$. The coefficient λ accounts for the fact that the absorptive cross section for the intermediate parton, c , may be different from that for the incoming particle (proton). Since the equations (3-5) describe the interaction amplitude and not the cross section we have a factor $1/2$ in the exponent. In terms of multi-Pomeron vertices, the absorption factors, $\exp(-\lambda\Omega_i(y, b)/2 - \lambda\Omega_k(y', b)/2)$, in (4,5) correspond to

$$g_m^n = n \cdot m \cdot \lambda^{n+m-2} g_N / 2 \quad \text{for } n + m \geq 3. \quad (6)$$

Note that, since the intermediate parton may be absorbed by the interaction with the particles (partons) from the wave function of both beam or target hadron, we now need to solve the two equations, (4) and (5). This is done iteratively. The resulting solution can then be used in the eikonal formulae to determine all soft pp interactions.

In comparison with our previous model [11], we now include a non-zero slope ($\alpha' \neq 0$) of the Pomeron trajectory. The incoming proton wave function is described by three Good-Walker eigenstates, that is we use a 3-channel eikonal for the rescattering of fast particles. The transverse size squared of each eigenstate is proportional to the corresponding absorptive cross section; $R_i^2 \propto \sigma_i$. That is we assume that the parton density at the origin is the same for each eigenstate. The shape of the Pomeron-nucleon vertex is parametrised by the form factor $V(t) = \exp(dt)/(1 - t/d_1)^2$, whose Fourier transform, $V(b)$, plays the role of the initial conditions for $\Omega(y = 0, b)$.

Next, we allow for four different t -channel states, which we label a : one for the secondary Reggeon (R) trajectory and three Pomeron states (P_1, P_2, P_3) to mimic the BFKL diffusion in the logarithm of parton transverse momentum, $\ln(k_t)$ [12]. To be precise, since the BFKL Pomeron [13] is not a pole in the complex j -plane, but a branch cut, we approximate the cut by three t -channel states of a different size. The typical values of k_t in each of the three states is about $k_{t1} \sim 0.5$ GeV, $k_{t2} \sim 1.5$ GeV and $k_{t3} \sim 5$ GeV. Thus the system (4,5) is replaced by

$$\frac{d\Omega_i^a(y, b)}{dy} = \exp(-\lambda\Omega_i(y, b)/2 - \lambda\Omega_k(y', b)/2) \left(\Delta^a + \alpha' \frac{d^2}{d^2b} \right) \Omega_i^a(y, b) + V_{aa'} \Omega_i^{a'} \quad (7)$$

$$\frac{d\Omega_k^a(y', b)}{dy'} = \exp(-\lambda\Omega_i(y, b)/2 - \lambda\Omega_k(y', b)/2) \left(\Delta^a + \alpha' \frac{d^2}{d^2b} \right) \Omega_k^a(y', b) + V_{aa'} \Omega_k^{a'}. \quad (8)$$

The transition factors $V_{aa'}$ were fixed by properties of the BFKL equation. In the exponents, the opacities Ω_i (Ω_k) are actually the sum of the opacities $\Omega_i^{a'}$ ($\Omega_k^{a'}$) with corresponding coefficients (see [14] for more details).

Clearly the number of parameters in such a model is large. Therefore, instead of a straightforward fit of the data, we adjust the majority of parameters in reasonable intervals and demonstrate that such a model allows us to reproduce all the available data on diffractive cross sections, σ_t , $d\sigma^{el}/dt$, $\sigma_{\text{low mass diss}}^{SD}$, $d\sigma^{SD}/dM^2$. The quality of the description is demonstrated in Fig.2, where we also present the prediction for elastic cross section at the LHC energy $\sqrt{s} = 14$ TeV.

The values of the parameters that we use are: $d = 0.15 \text{ GeV}^{-2}$, $d_1 = 1.5 \text{ GeV}^2$, $\lambda = 0.25$, $\alpha'_R = 0.9 \text{ GeV}^{-2}$, $\alpha_R(0) = 0.6$ and, for each of 3 components of the Pomeron, $\Delta^a = 0.3$. The Pomeron intercepts are consistent with the expectations of resummed NLL BFKL which gives $\omega_0 \equiv \alpha_P(0) - 1 \sim 0.3$ practically independent of the scale k_t [15]. The slopes of the Pomeron trajectories are: $\alpha'_{P_1} = 0.05 \text{ GeV}^{-2}$ for the large size Pomeron component, $\alpha'_{P_2} = 0.05/9 \text{ GeV}^{-2}$ for the second component ($\alpha' \propto 1/k_t^2$), and $\alpha'_{P_3} = 0$ for the smallest size Pomeron component.

This model, which we have tuned to describe the available data, allows us to predict, in principle, all features of soft pp high energy interactions. Let us consider the cross section for beam particle diffractive dissociation (with a rapidity gap up to y). First recall the usual eikonal relations

$$\sigma_t = 2 \int d^2b (1 - e^{\Omega(b)/2}); \quad \sigma_{el} = \int d^2b (1 - e^{-\Omega(b)/2})^2; \quad \sigma_{inel} = \int d^2b (1 - e^{-\Omega(b)}).$$

For each impact parameter point b , the desired cross section for single dissociation is proportional (i) to the elastic parton $c - k$ cross section $(1 - \exp(-\lambda\Omega_k(y, b)/2))^2$; (ii) to the probability to find the intermediate parton c in the interval dy , that is $\Delta \exp(-\lambda\Omega_i/2 - \lambda\Omega_k/2)$; (iii) to the amplitude Ω_i of the parton $c -$ beam interaction; (iv) to the gap survival factor $S^2(b) = \exp(-\Omega(Y, b))$ (where $Y = \ln s$). The resulting cross section reads

$$\begin{aligned} \frac{d\sigma^{SD}}{dy} = N \int d^2b_1 d^2b_2 (1 - e^{-\lambda\Omega_k(y, b_1)/2})^2 \Delta e^{-\lambda\Omega_i(Y-y, b_2)/2 - \lambda\Omega_k(y, b_1)/2} \times \\ \times \Omega_i(Y - y, b_2) e^{-\Omega(Y, \vec{b}_1 + \vec{b}_2)}, \end{aligned} \quad (9)$$

where b_1 (b_2) are the coordinates in the impact parameter plane with respect to the target (beam) hadron. Expression (9) must be averaged over the components (that is the Good-Walker eigenstates) of the beam and target hadrons and summed over the different t -channel states (R, P_1, P_2, P_3) with appropriate normalisation factors N . The energy behaviour of the diffractive cross sections, and of the multiplicities of the secondaries produced by the t -channel Pomeron components of different sizes, are shown in Fig.3.

Note that, starting with the same ‘bare’ intercepts ($\Delta = 0.3$), after the absorptive correction, the contribution of the large-size component becomes practically flat, while the small-size contribution, which is much less affected by the absorption, continues to grow with energy. Such a behaviour is consistent with experiment, where the density of low k_t secondaries is practically saturated, while the probability to produce a hadron with a large transverse momentum (say, more than 5 GeV) grows with the initial energy.

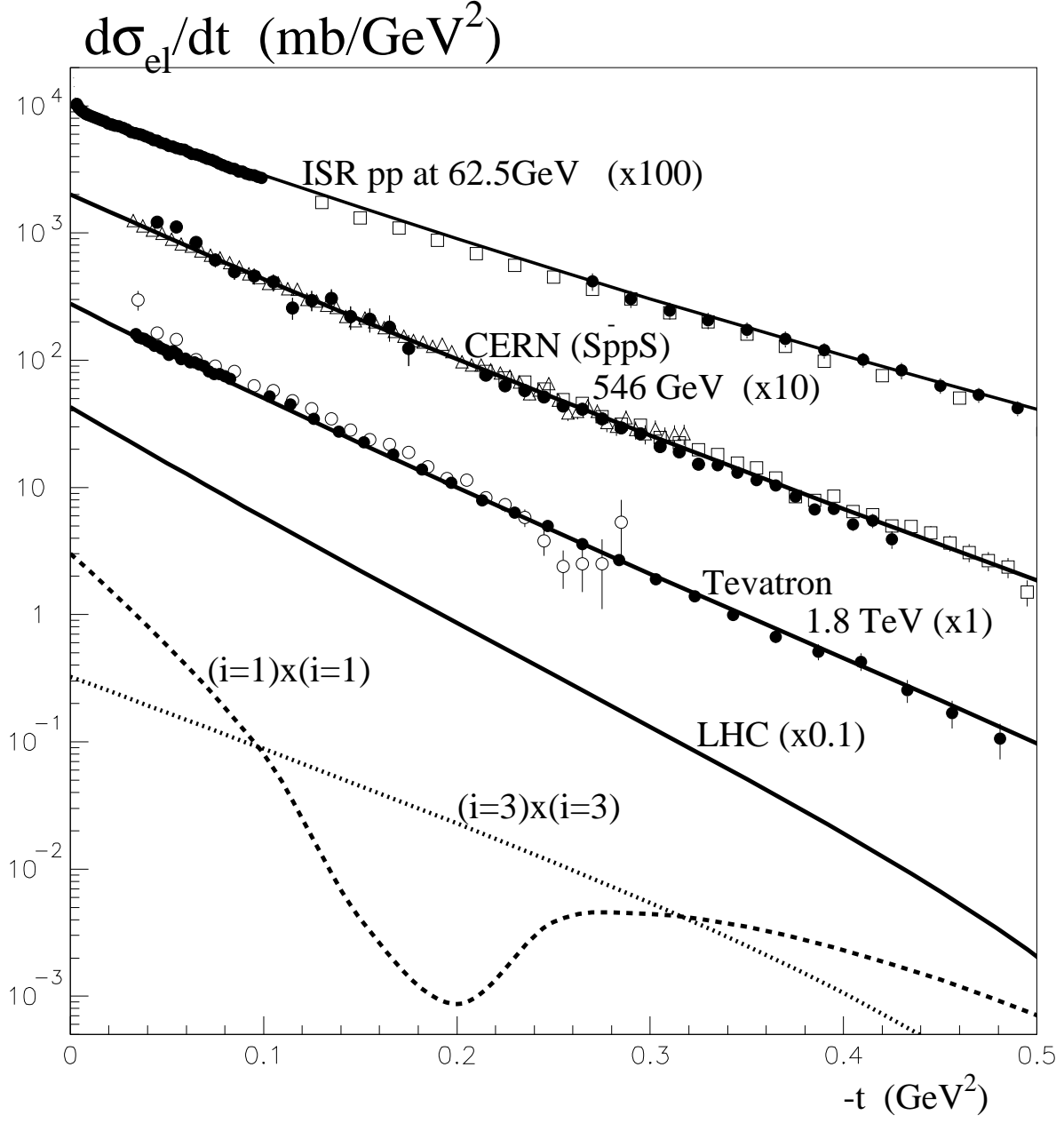


Figure 2: The description of the t dependence of the elastic pp cross section data. The dashed and dotted lines are the contributions at the LHC energy from the elastic scattering of the largest size ($i = 1$) and the smallest size ($i = 3$) components. Interestingly, we see that the complete set of eikonal contributions gives a smooth prediction for the elastic cross section in this t interval at the LHC energy.

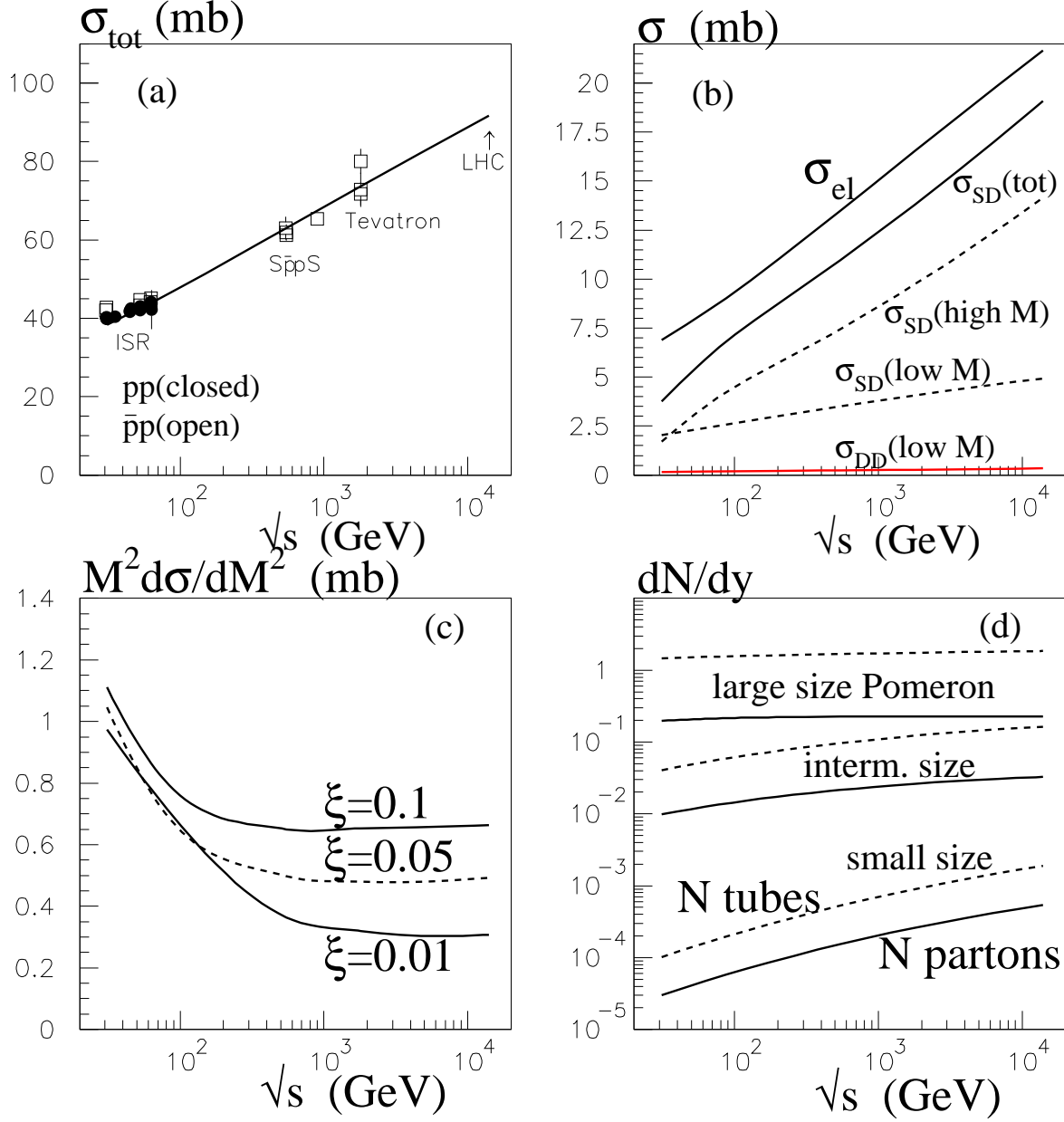


Figure 3: The energy dependence of (a) the total, (b) the elastic and diffractive dissociation, pp cross sections and (c) the cross sections of dissociation to a fixed M^2 state, where $\xi = M^2/s$. Plot (d) shows the parton multiplicity (solid lines) and the number of ‘colour tubes’ (dashed) produced by the Pomeron components of different size.

4 Conclusion

After accounting for absorptive effects the new triple-Regge analysis leads to a rather large triple-Pomeron vertex $g_{3P} = \lambda g_N$ with $\lambda \geq 0.2$. This indicates that in order to describe diffractive processes at the LHC we must use a model which includes multi-Pomeron interactions. We construct such a model in which the absorption of the intermediate partons is described by conventional-like factors $\exp(-\lambda\Omega)$. In terms of the multi-Pomeron vertices, this corresponds to $g_m^n = nm\lambda^{n+m-2}g_N/2$. The model reasonably well reproduces available diffractive data on σ_t , $d\sigma^{el}/dt$, $d\sigma^{SD}/dM^2$ using the parameters: $\Delta = 0.3$, $\alpha'_{Pom} = 0.05 \text{ GeV}^{-2}$, $\lambda = 0.25$. It thus leads to the hope that there is a smooth matching between the perturbative QCD treatment of the Pomeron and the multi-Pomeron description of soft interactions.

Since the screening corrections caused by the ‘enhanced’ multi-Pomeron diagrams, that is by the high-mass dissociation, slow down the growth of the cross section with energy, the model predicts a relatively low total cross section at the LHC energy, namely $\sigma_t(LHC) \simeq 90 \text{ mb}$ [11, 14]. Predictions for LHC soft interactions are shown in Figs. 2 and 3.

References

- [1] V.N. Gribov and A.A. Migdal, Sov. J. Nucl. Phys. **8** 583 (1969).
- [2] V.N. Gribov and A.A. Migdal, Sov. Phys. JETP **28** 784 (1969).
- [3] V.A. Khoze, A.D. Martin and M.G. Ryskin, Eur. Phys. J. **C23** 311 (2002).
- [4] V.A. Khoze, A.D. Martin and M.G. Ryskin, Eur. Phys. J. **C19** 477 (2001), erratum **C20** 599 (2001);
V.A. Khoze, A.D. Martin and M.G. Ryskin, arXiv:hep-ph/0006005.
- [5] M.L. Good and W.D. Walker, Phys. Rev. **120** 1857 (1960).
- [6] V.A. Abramovsky, V.N. Gribov and O.V. Kancheli, Sov. J. Nucl. Phys. **18** 308 (1973).
- [7] R.D. Field and G.C. Fox, Nucl. Phys. **B80** 367 (1974);
A.B. Kaidalov, V.A.Khoze, Yu.F. Pirogov and N.L. Ter-Isaakyan, Phys. Lett. **B45** 471 (1974);
for a review see A.B. Kaidalov, Phys. rep. **50** 157 (1979).
- [8] E.G.S. Luna, V.A. Khoze, A.D. Martin and M.G. Ryskin, arXiv:0807.4115.
- [9] J. Bartels, M.G. Ryskin and G.P. Vacca, Eur. Phys. J. **C27** 101 (2003).
- [10] ZEUS collaboration: Abstract 549, Int. Europhysics Conf. on HEP, Aachen, July 2003.
- [11] M.G. Ryskin, A.D. Martin and V.A. Khoze, Eur. Phys. J. **C54** 199 (2008).

- [12] L.N. Lipatov, Sov. Phys. JETP **63** 904 (1986).
- [13] V.S. Fadin, E.A. Kuraev, and L.N. Lipatov, Phys. Lett. B **60** (1975) 50;
 E.A. Kuraev, L.N. Lipatov, and V.S. Fadin, Zh. Eksp. Teor. Fiz. **71** (1976) 840 [Sov. Phys. JETP **44** 443 (1976)]; *ibid.* **72** (1977) 377 [**45** (1977) 199];
 I.I. Balitsky and L.N. Lipatov, Yad. Fiz. **28** (1978) 1597 [Sov. J. Nucl. Phys. **28** (1978) 822].
- [14] M.G. Ryskin, A.D. Martin and V.A. Khoze, to be published.
- [15] V.S. Fadin and L.N. Lipatov, Phys. Lett. **B429** (1998) 127;
 G. Camici and M. Ciafaloni, Phys. Lett. **B430** (1998) 349;
 G.P. Salam, JHEP **9807** 019 (1998), Act. Phys. Pol. **B30** 3679 (1999);
 M. Ciafaloni, D. Colferai and G.P. Salam, Phys. Lett. **B452** 372 (1999), Phys. Rev. **D60** 114036 (1999).